Structural Engineering and Mechanics, Vol. 7, No. 6 (1999) 561-573
DOI: http://dx.doi.org/10.12989/sem.1999.7.6.561

Convergence of the C^* family of finite elements and problems associated with forcing continuity of the derivatives at the nodes

B. Bigdeli† and D.W. Kelly‡

School of Mechanical and Manufacturing Engineering,
The University of New South Wales, Sydney, NSW 2052, Australia

Abstract. A C^*-convergence algorithm for finite element analysis has been proposed by Bigdeli and Kelly (1997) and elements for the first three levels applied to planar elasticity have been defined. The fourth level element for the new family is described in this paper and the rate of convergence for the C^*-convergence algorithm is investigated numerically. The new family adds derivatives of displacements as nodal variables and the number of nodes and elements can therefore be kept constant during refinement. A problem exists on interfaces where the derivatives are required to be discontinuous. This problem is addressed for curved boundaries and a procedure is suggested to resolve the excessive inter-element continuity which occurs.

Key words: stress analysis; the finite element method; nodal degrees of freedom; C^*-convergence.

1. Introduction

A new family of finite elements has been introduced by Bigdeli and Kelly (1996 and 1997). This family of higher-order quadrilaterals is primarily developed for the finite element analysis of plane elasticity problems, using the displacement method formulation. In this family the number of nodes and the number of elements are fixed, and refinement is achieved by adding derivatives of the nodal displacements as degrees of freedom at the nodes. The family has been called the C^* family of elements in which a superscript refers to the level of continuity of displacement and derivatives of displacement at the nodes. In the previous papers the first three elements of this family (i.e., the C^0, C^{1*} and C^{2*} elements) have been described and typical applications of the family have also been presented. The C^0 element enforces continuity only of displacements and is the standard 4-node finite element for planar elasticity. The C^{1*} element is the first new element and enforces continuity of the first derivatives of displacement at the nodes, etc.

In the previous work it was shown that the C^* family has elements equivalent to every second element in the p-family with the first four elements being linear, cubic, pentic and seventh order. However, the C^* family has degrees of freedom only at corner nodes where the sharing of degrees of freedom between elements is maximised. The C^* algorithm is therefore guaranteed to

† Dr. (formerly Ph.D student)
‡ Associate Professor

exhibit a faster rate of convergence than a p-convergence algorithm based, for example, on the serendipity family of elements if the necessary degree of discontinuity of derivatives is incorporated into the assembled finite element model.

In this paper the fourth element of the new family (i.e., the C^3* element) is described and the higher rate of convergence of the new approach is demonstrated.

A problem associated with these elements is that continuity of derivaties is enforced at the nodes, and this might not be correct if the node lies on an interface between regions with different thickness or material properties, or if the node is at a point of strain singularity. Bigdeli and Kelly (1997) have proposed a solution in which multiple nodes are defined at these points and Lagrange multipliers used to enforce continuity of only those parameters which are required to be continuous at the nodes. In this paper we generalise the formulation for curved boundaries and apply the procedures to a reinforced hole. Convergence for Mode I loading on a crack is also considered to demonstrate the flexibility of the approach.

2. Derivation of the C^3* element shape functions

Fig. 1 shows first four members of the family of C* elements. The derivation of elements 1 to 3 and an associated isoparametric mapping is discussed by Bigdeli and Kelly (1996, 1997), Bigdeli (1996). The fourth element of the C* family is a four-node quadrilateral element with 80 degrees of freedom. According to Fig. 1 there are ten degrees of freedom in each coordinate direction per node (i.e., U, $\frac{\partial U}{\partial \xi}$, $\frac{\partial U}{\partial \eta}$, $\frac{\partial^2 U}{\partial \xi^2}$, $\frac{\partial^2 U}{\partial \eta^2}$, $\frac{\partial^2 U}{\partial \xi \partial \eta}$, $\frac{\partial^3 U}{\partial \xi^3}$, $\frac{\partial^3 U}{\partial \xi^2 \partial \eta}$, $\frac{\partial^3 U}{\partial \xi \partial \eta^2}$, $\frac{\partial^3 U}{\partial \eta^3}$).

A polynomial which could be used to accommodate 40 d.o.f.'s in each coordinate direction for this element would be,

$$\begin{aligned} U = {} & a_1 + a_2\xi + a_3\eta + a_4\xi^2 + a_5\xi\eta + a_6\eta^2 + a_7\xi^3 + a_8\xi^2\eta + a_9\xi\eta^2 \\ & + a_{10}\eta^3 + a_{11}\xi^4 + a_{12}\xi^3\eta + a_{13}\xi^2\eta^2 + a_{14}\xi\eta^3 + a_{15}\eta^4 \\ & + a_{16}\xi^5 + a_{17}\xi^4\eta + a_{18}\xi^3\eta^2 + a_{19}\xi^2\eta^3 + a_{20}\xi\eta^4 \\ & + a_{21}\eta^5 + a_{22}\xi^6 + a_{23}\xi^5\eta + a_{24}\xi^4\eta^2 + a_{25}\xi^3\eta^3 \\ & + a_{26}\xi^2\eta^4 + a_{27}\xi\eta^5 + a_{28}\eta^6 + a_{29}\xi^7 + a_{30}\xi^6\eta \\ & + a_{31}\xi^5\eta^2 + a_{32}\xi^4\eta^3 + a_{33}\xi^3\eta^4 + a_{34}\xi^2\eta^5 \\ & + a_{35}\xi\eta^6 + a_{36}\eta^7 + a_{37}\xi^7\eta + a_{38}\xi^5\eta^3 \\ & + a_{39}\xi^3\eta^5 + a_{40}\xi\eta^7 \end{aligned} \tag{1}$$

where ξ and η are the intrinsic coordinates $-1 \leq \xi,\ \eta \leq -1$ on the square which is to be mapped to the real element geometry.

For this element the displacement field is a complete polynomial of degree seven with four extra terms of degree eight. In order to calculate the 40 constants in Eq. (1), first the derivatives $\frac{\partial U}{\partial \xi}$, $\frac{\partial U}{\partial \eta}$, $\frac{\partial^2 U}{\partial \xi^2}$, $\frac{\partial^2 U}{\partial \eta^2}$, $\frac{\partial^2 U}{\partial \xi \partial \eta}$, $\frac{\partial^3 U}{\partial \xi^3}$, $\frac{\partial^3 U}{\partial \xi^2 \partial \eta}$, $\frac{\partial^3 U}{\partial \xi \partial \eta^2}$, $\frac{\partial^3 U}{\partial \eta^3}$ should be taken. Then substituting for ξ and η with their corresponding nodal values (i.e., -1 or 1), a system of 40 equations with 40 unknown constants (i.e., a_1 to a_{40}) is constructed. On solving for the unknowns (using, for example MATLAB 1992), appropriate shape functions in local coordinates (ξ, η) are derived

which have been reported in Bigdeli (1996).

In general,

$$N_i = f_i(\xi,\ \eta) \qquad (i=1,\ ...,\ 40) \tag{2}$$

and,

$$U = \sum_{i=1}^{40} N_i U_i \tag{3}$$

where the nodal degree of freedom set in the first coordinate direction is given by,

$$U^T = \left\{ \begin{array}{l} U_1 \dfrac{\partial U}{\partial \xi}\Big|_1 \ \dfrac{\partial U}{\partial \eta}\Big|_1 \ \dfrac{\partial^2 U}{\partial \xi^2}\Big|_1 \ \dfrac{\partial^2 U}{\partial \eta^2}\Big|_1 \ \dfrac{\partial^2 U}{\partial \xi \partial \eta}\Big|_1 \\ \dfrac{\partial^3 U}{\partial \xi^3}\Big|_1 \ \dfrac{\partial^3 U}{\partial \xi^2 \partial \eta}\Big|_1 \ \dfrac{\partial^3 U}{\partial \xi \partial \eta^2}\Big|_1 \ \dfrac{\partial^3 U}{\partial \eta^3}\Big|_1, \ ..., \\ ...,\ U_4 \dfrac{\partial U}{\partial \xi}\Big|_4 \ \dfrac{\partial U}{\partial \eta}\Big|_4 \ \dfrac{\partial^2 U}{\partial \xi^2}\Big|_4 \ \dfrac{\partial^2 U}{\partial \eta^2}\Big|_4 \ \dfrac{\partial^2 U}{\partial \xi \partial \eta}\Big|_4 \\ \dfrac{\partial^3 U}{\partial \xi^3}\Big|_4 \ \dfrac{\partial^3 U}{\partial \xi^2 \partial \eta}\Big|_4 \ \dfrac{\partial^3 U}{\partial \xi \partial \eta^2}\Big|_4 \ \dfrac{\partial^3 U}{\partial \eta^3}\Big|_4 \end{array} \right\}. \tag{4}$$

A similar expression can be written in the other coordinate direction (i.e., V).

The element stiffness matrix $[k^e]$ in its local coordinate system $(\xi,\ \eta)$ is defined by,

$$[k^e] = \int_{A^e} [B]^T\ [D]\ [B]\ td\ (\text{area}) \tag{5}$$

in which $[D]$ is an elasticity matrix containing the appropriate material properties, and matrix $[B]$ contains the derivatives of shape functions with respect to X and Y, and would be a 3×80 matrix.

Eq. (5) is numerically integrated, by means of a Gaussian quadrature formula, over the entire element area in the element intrinsic coordinate system $(\xi,\ \eta)$. The derivatives in the nodal variable set remain defined in terms of the intrinsic coordinates. Prior to assembly the stiffness matrix and load vector are transformed so that derivatives are taken with respect to the global coordinates X and Y.

3. The rate of convergence

Establishing the superior rate of convergence of the C^*-convergence algorithm for a uniform refinement requires only establishing the reduced number of degrees of freedom compared to the uniform p-refinement. This has been done in Bigdeli and Kelly (1997) where reductions in the number of degrees of freedom by factors of 0.6 and 0.57 are determined for simple rectangular regions in two and three dimensions. The nodes in the new procedure exist only at the corners of the elements and therefore the sharing of degrees of freedom between neighboring elements is maximised. Because the new family is equivalent to each second member in a p-convergence family, convergence can be established from the p-convergence results. Superiority over the h-

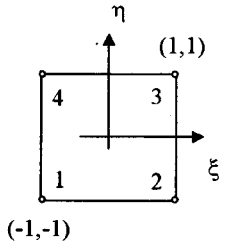

$U,\ V$

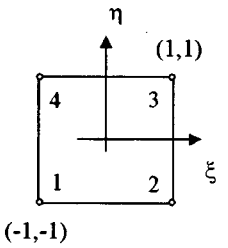

$$U,\ V$$

$$\frac{\partial U}{\partial \xi},\ \frac{\partial U}{\partial \eta}$$

$$\frac{\partial V}{\partial \xi},\ \frac{\partial V}{\partial \eta}$$

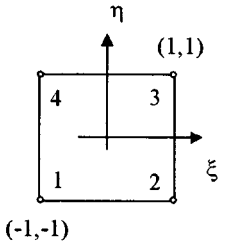

$$U,\ V$$

$$\frac{\partial U}{\partial \xi},\ \frac{\partial U}{\partial \eta},\ \frac{\partial^2 U}{\partial \xi^2},\ \frac{\partial^2 U}{\partial \eta^2},\ \frac{\partial^2 U}{\partial \xi \partial \eta}$$

$$\frac{\partial V}{\partial \xi},\ \frac{\partial V}{\partial \eta},\ \frac{\partial^2 V}{\partial \xi^2},\ \frac{\partial^2 V}{\partial \eta^2},\ \frac{\partial^2 V}{\partial \xi \partial \eta}$$

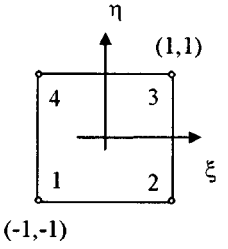

$$U,\ V$$

$$\frac{\partial U}{\partial \xi},\ \frac{\partial U}{\partial \eta},\ \frac{\partial^2 U}{\partial \xi^2},\ \frac{\partial^2 U}{\partial \eta^2},\ \frac{\partial^2 U}{\partial \xi \partial \eta},\ \frac{\partial^3 U}{\partial \xi^3},\ \frac{\partial^3 U}{\partial \xi^2 \partial \eta},\ \frac{\partial^3 U}{\partial \xi \partial \eta^2},\ \frac{\partial^3 U}{\partial \eta^3}$$

$$\frac{\partial V}{\partial \xi},\ \frac{\partial V}{\partial \eta},\ \frac{\partial^2 V}{\partial \xi^2},\ \frac{\partial^2 V}{\partial \eta^2},\ \frac{\partial^2 V}{\partial \xi \partial \eta},\ \frac{\partial^3 V}{\partial \xi^3},\ \frac{\partial^3 V}{\partial \xi^2 \partial \eta},\ \frac{\partial^3 V}{\partial \xi \partial \eta^2},\ \frac{\partial^3 V}{\partial \eta^3}$$

Fig. 1 Four levels of the C^* family of elements

convergence method is also established in the *p*-convergence literature.

To demonstrate the result, consider the stress singularity at the corner of an *L*-shaped domain. This problem has become a standard problem to investigate the rate of convergence of different schemes in the finite element method. It was considered in Bigdeli and Kelly (1997) where the results reported here for the first three elements in the new family were reported. Gago (1982) also worked on this problem to develop an *a*-posteriori error analysis and a part of his results will be used in this study. He used an irregular mesh to demonstrate the efficiency of the *adaptive p*-convergence algorithm based on the *a*-posteriori error estimate developed in his work. In this study, however, we are not concerned about the adaptivity technique in the finite element method. Therefore, a regular mesh will be analysed only, and the adaptivity in the C^*-convergence procedure is left for future investigations.

The geometry and loading condition for this problem are shown in Fig. 2. The plane stress condition is assumed with a Poisson's ratio of 0.3. Starting from a uniform mesh consisting of 27

elements and refining the mesh uniformly for an *h*-convergence scheme, a set of meshes containing 27, 108 and 432 elements is constructed. To build a series of solutions for a *p*-convergence scheme, the number of elements is fixed to 27 and a sequence of meshes consisting of linear, quadratic, cubic and finally quartic elements is produced. In a similar fashion a series of meshes consisting of C^0 linear, the C^{1*} cubic the C^{2*} pentic and C^{3*} seventh order elements of the C^* family is constructed.

If it is possible to assume that,

$$\text{error} = C\left(\frac{1}{ndof}\right)^n \tag{6}$$

in which *ndof* is the total number of d.o.f.'s in the mesh, and C and n are two constants. Then on a logarithmic scale we have,

$$\log(\text{error}) = \log C + n \log\left(\frac{1}{ndof}\right) \tag{7}$$

Therefore, the slope (i.e., n) of a curve plotted as log(error) versus log(1/*ndof*) will provide the rate of convergence for different refinement schemes. The most common parameter to use in this study is the error in *strain energy*. This norm is defined as,

$$\log \| e \|^2 = \log (\| u \|_E^2 - \| u \|_{FE}^2) \tag{8}$$

in which $\| u \|_E^2$ is 'exact solution' for twice the strain energy for the *L*-shaped domain in Fig. 2 obtained through very refined mesh and Richardson's extrapolation, and $\| u \|_{FE}^2$ is twice the strain energy of the finite element solution.

Gago (1982) reported $\| u \|_E$=5.58. However a figure with two decimal digits accuracy was found to be unsatisfactory for the high accuracy solutions being achieved here. A series of meshes consisting of 8-node quadratic elements using the STRAND6 (1993) finite element package was constructed with up to 12000 elements. Results for the Richardson's extrapolation for the exact solution gave $\| u \|_E$=5.58015, and consequently $\| u \|_E^2$=31.13807 has been chosen as the 'exact solution'. At the end of each finite element solution the transpose of the computed nodal

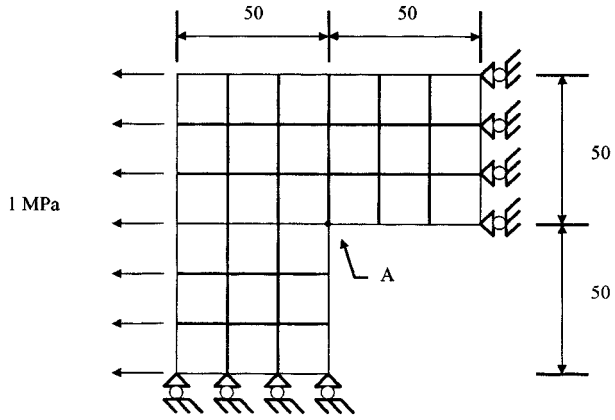

Fig. 2 Geometry, loading and boundary conditions for the *L*-shaped domain (E=1000, ν=0.3, t=0.1)

displacement vector is multiplied by the nodal load vector to produce the solution strain energy. The convergence behavior of different refinement schemes, for a 27 element initial mesh, is depicted in Fig. 3. The superiority of the C^*-convergence over the h- and p-convergence schemes is revealed.

Although it is possible to predict a convergence rate for the C^* family of elements as an average slope of the corresponding curve in Fig. 3, the C^3*-element is included in this test in Fig. 4. This figure shows the results obtained for a series of meshes based on a starting configuration of three elements. In Szabo and Babuska (1991) the asymptotic convergence rate for the p-version applied to this problem is given, and it is reported that the method does not enter the asymptotic convergence mode until p=7. The final convergence rate for the p-convergence is reported to be

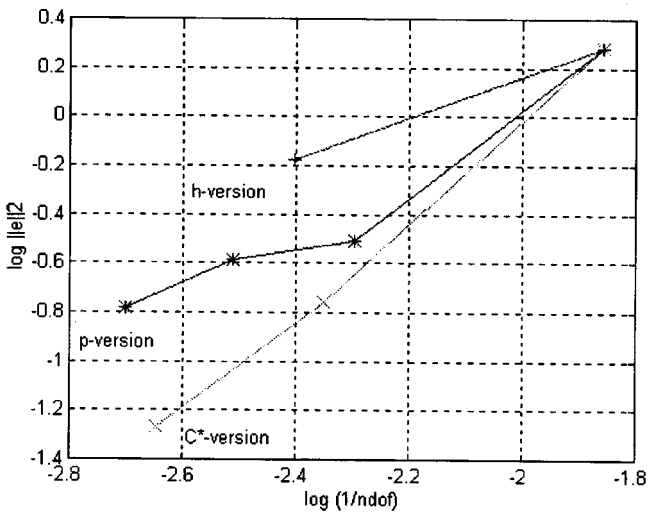

Fig. 3 Rate of convergence for the L-shaped domain (27 elements)

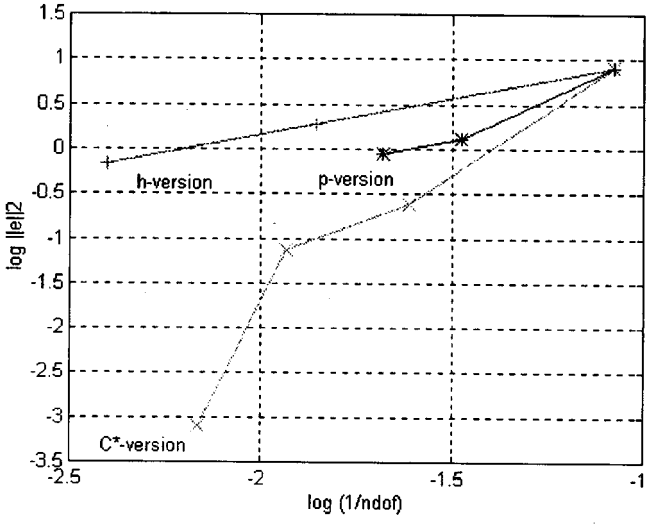

Fig. 4 Rate of convergence for the L-shaped domain (3 elements)

0.558.

Gago (1982) reported a rate of convergence for low order elements in the *h*-version, in a regular mesh, equal to 0.7, and a rate of convergence for the *p*-version, as an average slope of the corresponding curve, equal to 1.3. In other words he has shown that the initial rate of convergence of the *p*-version is twice that of the *h*-version.

An average slope for the C^*-convergence scheme, as shown in Fig. 4, is about 2.89. In other words the initial rate of convergence of the C^*-refinement scheme is more than four times that of the *h*-version, and twice that of the *p*-version.

4. Application to mode I loading of a crack

This problem was also reported in Bigdeli and Kelly (1997) for the first three elements in the new family. A difficulty which must be addressed for problems with singularities is that strains can be discontinuous at the crack tip and therefore forcing continuity will reduce convergence of the algorithm. We consider here an example of Mode I loading on a cracked specimen.

Table 1 compares the error in the strain energy for meshes of 4 elements. The "exact" strain energy has been generated by extrapolation from a sequence of refined meshes of C^0 4-node elements (using up to 25600 elements). In the first column the derivatives are forced to be continuous at the crack tip and an artificial smoothing of the strain field occurs. In the second column 4 nodes are defined at the crack tip and continuity of displacements *u, v* alone is enforced at that point.

5. Discontinuous derivatives on curved boundaries

To extend the procedure described in the previous work by Bigdeli and Kelly to include an interface between curved regions with different thickness, a quarter of a reinforced hole, as shown in Fig. 6, is considered.

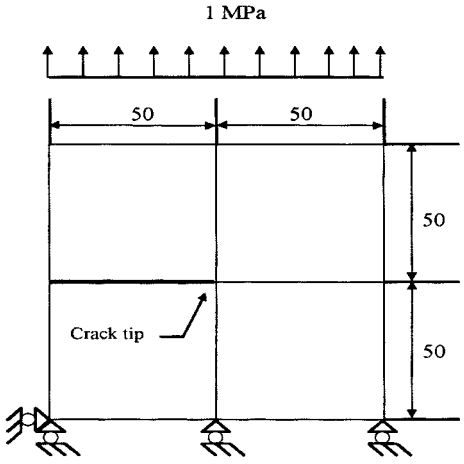

Fig. 5 Mode I loading of a crack (E=1000, ν=0.3, t=0.1)

Table 1 Remedy for strain smoothing at the crack tip (Lagrange multiplier approach). (Exact solution for strain energy=0.46235)

Element type	% error in strain energy (corner derivatives continuous)	% error in strain energy (corner derivatives discontinuous)
C^0 4-node	45.34	45.34
C^{1*} 4-node	35.98	7.77
C^{2*} 4-node	13.54	0.9
C^{3*} 4-node	4.48	0.06

The initial finite element mesh which consists of 6 elements is shown in Fig. 7. A series of meshes consisting of 6, 24, 96 and 384 C^0 8-node elements, using the STRAND6 (1993) finite element system, has been constructed and stress results for point A are presented in Table 2. Stresses for point A for a mesh consisting of 6 C^{1*} elements are also shown in this table. We notice that the stresses recovered at point A are, in fact, average values obtained from neighboring elements.

It is expected that a mesh consisting of C^{1*} elements, when modified to release the excessive continuity, will produce discontinuous stresses at point A. It is also to be noted that recovery of stresses using the standard C^0 elements requires post-processing of element results. In the new procedure strains are available directly at the nodes and stresses are recovered with minimal post-processing.

To allow discontinuous values of derivatives to occur at the interface where the thickness

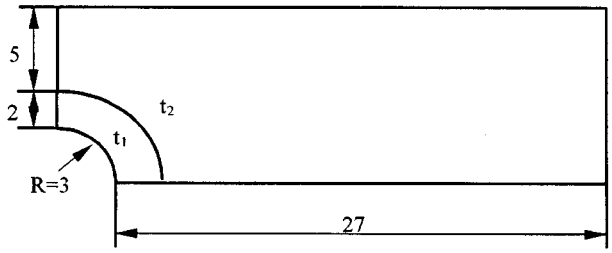

Fig. 6 A quarter of a reinforced hole (t_1=2t_2)

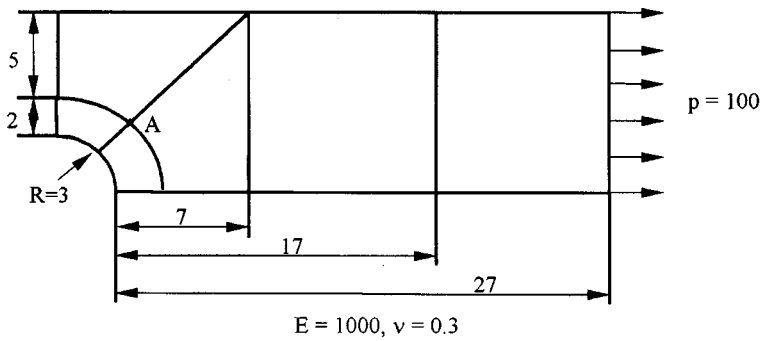

E = 1000, ν = 0.3

Fig. 7 Finite element model of a reinforced hole under constant tenson (t_1=0.2 and t_2=0.1)

Table 2 Stress results for point A shown in Fig. 7

Element type	No. of elements	No. of d.o.f	σ_{XX} (MPa)	σ_{YY} (MPa)	σ_{XY} (MPa)
C^0 8-node	6	62	87.526	-2.082	-7.452
C^0 8-node	24	194	104.975	-19.807	-7.386
C^0 8-node	96	674	108.329	-23.124	-7.722
C^0 8-node	384	2498	109.554	-24.358	-7.837
C^1* 4-node	6	78	96.182	-21.614	-7.184

varies, a procedure was devised (Bigdeli and Kelly 1996, Bigdeli 1996) in which two nodes are defined on the interface, and Lagrange multipliers are used to constrain those nodal degrees of freedom which should be continuous across the interface. The relations between derivatives of displacements at the interface exist only when they are considered in the normal and tangential (n, t) coordinate system. For this reason, first, a coordinate transformation should be established

According to Fig. 8 the following relationships between two coordinate systems exist (Tsai and Hahn 1980),

$$x = (\cos\theta)\, n - (\sin\theta)\, t$$
$$y = (\sin\theta)\, n + (\cos\theta)\, t \tag{9}$$

and a similar expression can be written for displacements as,

$$u = (\cos\theta)\, u_n - (\sin\theta)\, v_n$$
$$v = (\sin\theta)\, u_n + (\cos\theta)\, v_n \tag{10}$$

in which u and v are displacement components in the Cartesian (x, y) coordinate system, and u_n and v_n are displacement components in the (n, t) coordinate system. Differentiating Eq. (10) with respect to the (x, y) coordinate system, and using the chain rule will produce appropriate relations between derivatives of displacement in the two coordinate systems as follows,

$$\frac{\partial u}{\partial x} = \frac{\partial u_n}{\partial n} C^2 - \frac{\partial v_n}{\partial n} SC - \frac{\partial u_n}{\partial t} SC + \frac{\partial v_n}{\partial t} S^2 \tag{11a}$$

$$\frac{\partial v}{\partial x} = \frac{\partial u_n}{\partial n} SC + \frac{\partial v_n}{\partial n} C^2 - \frac{\partial u_n}{\partial t} S^2 - \frac{\partial v_n}{\partial t} CS \tag{11b}$$

$$\frac{\partial u}{\partial y} = \frac{\partial u_n}{\partial n} SC - \frac{\partial v_n}{\partial n} S^2 + \frac{\partial u_n}{\partial t} C^2 - \frac{\partial v_n}{\partial t} SC \tag{11c}$$

$$\frac{\partial v}{\partial y} = \frac{\partial u_n}{\partial n} S^2 + \frac{\partial v_n}{\partial n} SC + \frac{\partial u_n}{\partial t} SC + \frac{\partial v_n}{\partial t} C^2 \tag{11d}$$

in which S=sinθ and C=cosθ.

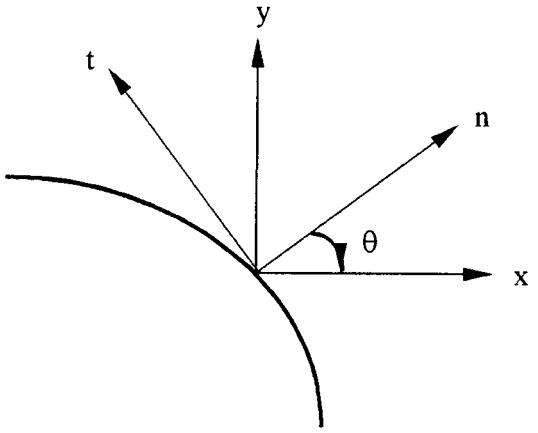

Fig. 8 The Cartesian (x, y) and the normal and tangential (n, t) coordinate systems

Eqs. (11a) to (11d) can be written in a matrix form as follows,

$$\begin{bmatrix} u \\ v \\ \frac{\partial u}{\partial x} \\ \frac{\partial v}{\partial x} \\ \frac{\partial u}{\partial y} \\ \frac{\partial v}{\partial y} \end{bmatrix} = \begin{bmatrix} C & -S & 0 & 0 & 0 & 0 \\ S & C & 0 & 0 & 0 & 0 \\ 0 & 0 & C^2 & -SC & -SC & S^2 \\ 0 & 0 & SC & C^2 & -S^2 & -SC \\ 0 & 0 & SC & -S^2 & C^2 & -SC \\ 0 & 0 & S^2 & SC & SC & C^2 \end{bmatrix} \begin{bmatrix} u_n \\ v_n \\ \frac{\partial u_n}{\partial n} \\ \frac{\partial v_n}{\partial n} \\ \frac{\partial u_n}{\partial t} \\ \frac{\partial v_n}{\partial t} \end{bmatrix} \tag{12}$$

or,

$$\{u\} = [T]\ \{u_n\} \tag{13}$$

in which $\{u\}$ and $\{u_n\}$ are nodal degree of freedom sets in the (x, y) and (n, t) coordinate systems respectively, and $[T]$ is the transformation matrix.

Having produced the transformation matrix $[T]$, the following two step procedure can be used to solve the stress smoothing problem for curved boundaries using the C^{1*} element.

First, nodal degrees of freedom corresponding to the points lying on the curve boundary (e.g., point A in Fig. 7) should be transformed to the (n, t) coordinate system by means of the transformation matrix $[T]$. We notice that there are two nodes corresponding to point A in the finite element mesh. One belongs to elements with thickness t_1 and one belongs to elements with thickness t_2.

In the second step, the following constraints are applied to those degrees of freedom by means of Lagrange multipliers described by Bigdeli and Kelly (1996), Bigdeli (1996).

$$u_n|_{t_1} - u_n|_{t_2} = 0$$
$$v_n|_{t_1} - v_n|_{t_2} = 0$$

$$\frac{\partial u_n}{\partial t}|_{t_1} - \frac{\partial u_n}{\partial t}|_{t_2} = 0$$
$$\frac{\partial v_n}{\partial t}|_{t_1} - \frac{\partial v_n}{\partial t}|_{t_2} = 0 \tag{14}$$

The procedure has been applied to the problem shown in Fig. 7 with a mesh consisting of 6 C^1* elements. As expected, discontinuous global stresses at point A are produced as: global stress at point A on element with thickness t_1=0.2 mm, $(\sigma_{XX}|_A)_{t_1}$=61.280 (MPa), and global stress at point A on element with thickness t_2=0.1 mm, $(\sigma_{XX}|_A)_{t_2}$=120.190 (MPa).

The average of these two stresses is not exactly the average reported in Table 2. The result in Table 2 corresponds to strains calculated at the nodes when elements are assembled with common nodal degrees of freedom.

It can be seen that the ratio between these values is inversely proportional to the thickness ratio in neighboring elements.

In order to generalised the result for any arbitrary point on the curved boundaries, a refined mesh consisting of 96 elements is produced. Discontinuous X-stresses (i.e., global stresses) for a mesh consisting of C^0-8 node elements are produced by extrapolation of Gauss point stresses to the common nodes and averaging those belonging to the elements with the same thickness. For the mesh consisting of C^1*-elements however, the two step procedure established in this study is employed. Results of this study for nodes on the curved boundary at angles 0°, 45° and 90° are depicted in Figs. 9 to 11 respectively. We note that at 90° the X-stress becomes the tangent stress. The discontinuity then only results from interaction with the normal strains factored by Poisson's ratio.

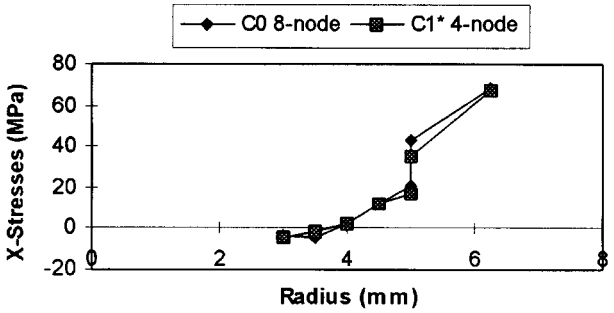

Fig. 9 Variation of X-stresses at θ=0°

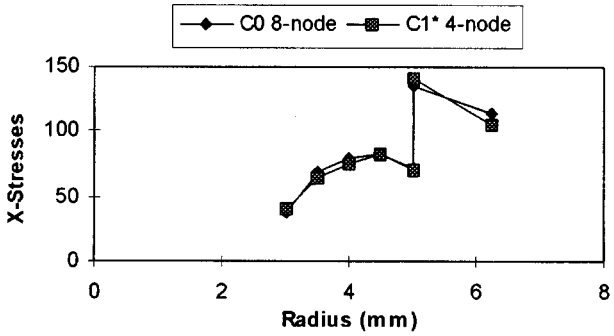

Fig. 10 Variation of X-stresses at θ=45°

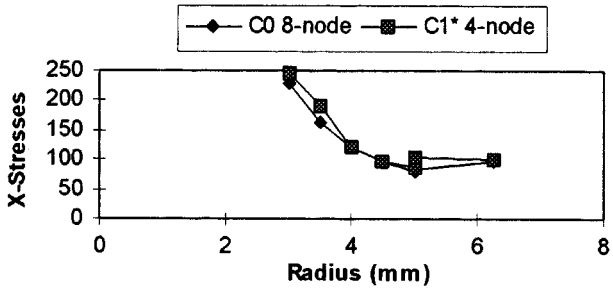

Fig. 11 Variation of X-stresses at θ=90°

6. Conclusions

The C^3* element, as the fourth level of the C* family of elements, has been developed and an average rate of convergence for this family established for coarse meshes on an L-shaped domain. The rate of convergence has been shown to be higher than that of the h- and p- convergence schemes. The results are also consistent with those reported in (Bigdeli and Kelly 1996, Bigdeli 1996, Bigdeli and Kelly 1997). The reasons for these higher rates of convergence are discussed in the introduction to this paper. A second important feature is that derivatives, and hence strains, are evaluated in the solution process and are available at nodes and therefore on the boundary of the domain. This is the location where they are often of most interest in engineering analysis.

The solution to the problem of excessive inter-element continuity between neighboring elements with different thickness discussed in the previous publications (Bigdeli and Kelly 1996, Bigdeli 1996, Bigdeli and Kelly 1997) is extended to include any arbitrary point on curved boundaries. The problem of Mode I loading on an edge crack for which strains are discontinuous at the singular point has also been considered.

Derivatives are also included as degrees of freedom in the Hermitian family of elements. The C* family differs from these elements in the application to planar elasticity and the fact that continuity of the derivatives is enforced only at the nodes.

Acknowledgements

The first author would like to thank the Ministry of Culture and Higher Education (MCHE) of the I. R. Iran for providing a scholarship which supported this research.

References

Bigdeli, B. and Kelly, D.W. (1996), "C*-convergence and nodal derivatives in the finite element method", *Proc. First Australasian Congress on Applied Mechanics*, The Institution of Engineers, Melbourne, Australia, **2**, 571-576.

Bigdeli, B. (1996), "An investigation of the C*-convergence in the finite element method", PhD. Thesis, The University of New South Wales, Sydney, Australia.

Bigdeli, B. and Kelly, D.W. (1997), "C*-convergence in the finite element method", *Int. J. Numer. Methods Engng.*, **40**, 4405-4425.

Gago, J.P. de S.R. (1982), "A-posteriori error analysis and adaptivity for the finite element method",

PhD. Thesis, Dept. of Civil Eng., University College of Swansea, Swansea, Wales.
MATLAB (1992), High-Performance Numeric Computation and Visualisation Software, User's Guide, The Math Works, Inc., 24 Prime Park Way, Natick, Mass. 01760, USA.
Tsai, S.W. and Hahn, H.T. (1980), "Introduction to composite materials", Technomic Publishing Co.
STRAND6 (1993) Finite Element Analysis System, Reference Manual and User Guide, G+D Computing Pty Ltd., Level 7, 541 Kent St., Sydney 2000, Australia.
Szabo, B. and Babuska, I. (1991), *Finite Element Analysis*, Wiley.